

## Molecular beam epitaxial growth window for high-quality (Ga,In)(N,As) quantum wells for long wavelength emission

Fumitaro Ishikawa,<sup>a)</sup> Michael Hörnicke, Uwe Jahn, Achim Trampert, and Klaus H. Ploog  
*Paul-Drude-Institut für Festkörperelektronik, Hausvogteiplatz 5-7, 10117 Berlin, Germany*

(Received 22 February 2006; accepted 23 March 2006; published online 11 May 2006)

We grow high-quality (Ga,In)(N,As) quantum wells containing 36% In and 4.5% N by molecular beam epitaxy, with a low As pressure and low substrate temperature growth concept. A V/III beam equivalent pressure ratio of 5 and a substrate temperature of 375 °C lead to highly regular ten-period multiple quantum well structures having abrupt interfaces and smooth surfaces. By varying the quantum well width from 4 to 8 nm, we observe 1.34–1.6  $\mu\text{m}$  emission of narrow linewidth ( $\leq 50$  meV) at room temperature after annealing. The large conduction band offset of 410 meV estimated from calculations is beneficial for a material system considered for high temperature laser operation. © 2006 American Institute of Physics. [DOI: 10.1063/1.2202113]

Quaternary (Ga,In)(N,As) is a material of great interest due to its band gap tunability and large conduction band offset with respect to GaAs. These properties are promising for the realization of low cost 1.55  $\mu\text{m}$  telecommunication lasers on GaAs substrate, which show good performance at high operation temperature.<sup>1,2</sup> Recently, lasers emitting at wavelengths above 1.5  $\mu\text{m}$  have been realized by molecular beam epitaxy (MBE) using (Ga,In)(N,As) or quinary (Ga,In)(N,As,Sb).<sup>3–5</sup> However, the growth process of these materials is still not well understood, especially for samples with quantum wells wider than 7 nm and containing large In and N amounts that are required for emission above 1.5  $\mu\text{m}$ . The major difficulties are (i) maintaining the two-dimensional growth mode, (ii) incorporating N at large In contents, and (iii) avoiding degradation of the material quality with increasing N concentration.<sup>3</sup>

(Ga,In)(N,As) is commonly grown at 420–450 °C with a V/III beam equivalent pressure (BEP) ratio of 15–50.<sup>3,4</sup> Under these conditions, (Ga,In)(N,As) quantum wells (QWs) containing more than 30% In easily roughen at the growth front. This is due to microscopic phase segregation and strain relaxation, which occurs at a critical layer thickness. In order to prevent these processes, a modification of the growth by the surfactant Sb has been employed.<sup>3,4</sup> In contrast, the recently achieved 1.5  $\mu\text{m}$  laser without Sb was grown at extremely different growth conditions: almost stoichiometric supply of group III and V elements and a low growth temperature of 350 °C.<sup>5</sup> Possible explanations for this result are the following: (i) the low growth temperature prevents strain relaxation, leading to abrupt heterointerfaces;<sup>6,7</sup> (ii) reducing the As pressure increases the surface diffusion length of group III adatoms counteracting the effect of the low temperature, as investigated in earlier MBE studies for the GaAs/(Al,Ga) system;<sup>8–11</sup> and (iii) the low As pressure allows the introduction of large amount of N in the layers due to the reduced competition for incorporation of group V elements.<sup>12</sup> Therefore, exploring the MBE growth conditions towards the low As pressure and low temperature regime is crucial in order to obtain high-quality (Ga,In)(N,As) layers with emission above 1.5  $\mu\text{m}$ . In this letter, we focus on the growth of (Ga,In)(N,As) multiple quantum wells (MQWs)

with large In and N contents using a V/III BEP ratio of 5 at a substrate temperature lower than 400 °C.

The MBE growth was carried out on semi-insulating GaAs(001) substrates. Conventional solid-source effusion cells were used for Ga and In, and an As-valved cracker cell was operated in the As<sub>4</sub> mode. Nitrogen was supplied by an ADDON rf plasma source. The substrate temperature during growth was monitored with a thermocouple, which has been calibrated by combining the GaAs oxide desorption temperature of 580 °C, the In melting point of 160 °C, and the transition points of reflection high-energy electron diffraction (RHEED) patterns.<sup>13</sup> Prior to the growth of the (Ga,In)  $\times$  (N,As)/Ga(N,As) MQW, a 300 nm thick undoped GaAs buffer layer was grown at 560 °C. For the growth of the MQW, the fluxes of all the elements were fixed throughout this study. A low As BEP of  $8 \times 10^{-7}$  Torr was used, which corresponds to a V/III BEP ratio of 5. The atomic V/III flux ratio was estimated to be 3. The growth rates were 0.24  $\mu\text{m}/\text{h}$  for the Ga(N,As) barriers and 0.4  $\mu\text{m}/\text{h}$  for the (Ga,In)(N,As) QWs. The In content was kept at 36%. The N concentration was kept slightly higher than 4% by assuming an identical incorporation for the ternary and quaternary materials. The Ga(N,As) barriers were grown by closing the shutters of both the In and the N cells in order to obtain a large band offset.<sup>1</sup> However, a small amount of about 0.8% N was incorporated into the GaAs layers in our case, due to the residual amount of atomic N diffusing into the growth chamber around the closed shutter.

The layers were characterized by high-resolution x-ray diffraction (XRD) with a simulation based on the dynamical diffraction theory<sup>14</sup> and reciprocal space mapping for an asymmetric reflection. The structural and morphological properties were investigated by transmission electron microscopy (TEM) and atomic force microscopy (AFM). The optical properties were investigated by cathodoluminescence (CL) equipped with a Hamamatsu R5509-72 photomultiplier which allows detection of CL up to 1.7  $\mu\text{m}$ . All measured spectra were corrected for the system response.

First, we carried out RHEED investigations to analyze the effect of the substrate temperature on the growth front. The (Ga,In)(N,As) growth surface was monitored just after the growth of 3 nm in the temperature range between 320 and 450 °C. Figure 1 shows the observed RHEED images. A

<sup>a)</sup>Electronic mail: ishikawa@pdi-berlin.de

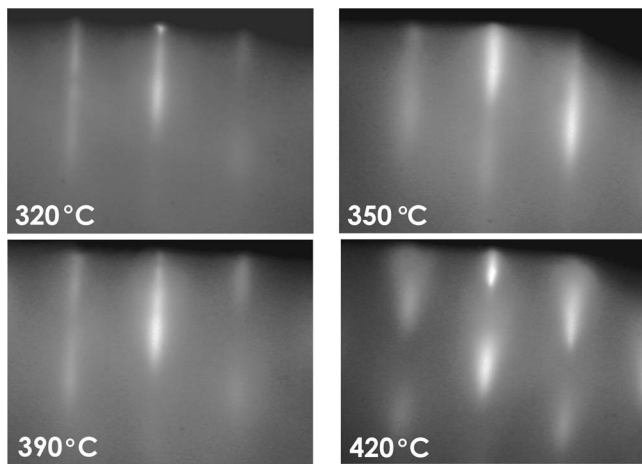


FIG. 1. RHEED patterns along the  $[1\bar{1}0]$  direction during the growth of 3 nm  $\text{Ga}_{0.6}\text{In}_{0.4}\text{N}_{0.04}\text{As}_{0.96}$  for the respective temperatures at a V/III BEP ratio of 5.

comparatively bright and streaky pattern was observed at temperatures between 350 and 390 °C. In contrast, the pattern becomes dim at lower temperatures. On the other hand, a roughening of the surface is observed at temperatures above 420 °C. The preferable growth temperature is about 50 °C lower than commonly used values.<sup>4</sup> The thickness of 3 nm is presumably lower than the critical thickness and strain relaxation has not yet occurred.<sup>4,9</sup> Therefore, the roughening probably results from the incongruent sublimation of As from the growth front due to the low As pressure, which disturbs the layer by layer growth. Consequently, the optimal growth temperature must be correspondingly reduced.<sup>8,9</sup>

The above interpretation was examined by growing a MQW structure consisting of ten periods of  $[(\text{Ga},\text{In})(\text{N},\text{As})$  (4 nm)/ $\text{Ga}(\text{N},\text{As})$  (11 nm)] at a substrate temperature of 375 °C. A bright and streaky RHEED pattern was observed throughout the growth, and a clear  $2 \times 3$  reconstruction appeared during the growth of the barriers.<sup>13</sup> Figure 2 displays an  $\omega$ - $2\theta$  XRD profile across the  $\text{GaAs}(004)$  reflection for this sample. The XRD profile exhibits satellite peaks with clearly resolved eight interference fringes stemming from the ten-period MQW structure, which demonstrates abrupt interfaces and a high periodicity of the MQW.<sup>15</sup> The simulated profile

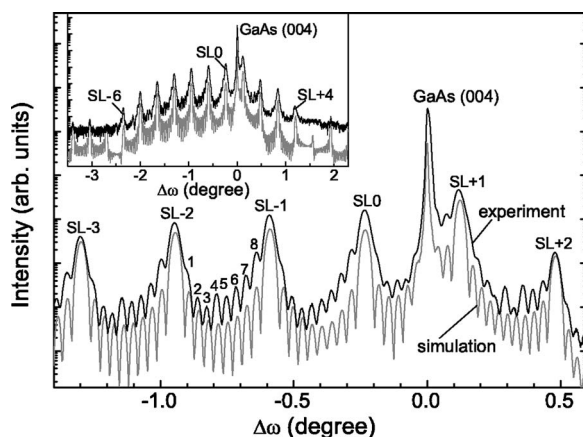


FIG. 2. Experimental and simulated XRD  $\omega$ - $2\theta$  scans of the  $[(\text{Ga},\text{In})(\text{N},\text{As})$  (4 nm)/ $\text{Ga}(\text{N},\text{As})$  (11 nm)] ten-period MQW across the  $\text{GaAs}(004)$  reflection. The MQW satellites are denoted by  $\text{SL}(\pm n)$ . The compositions obtained from the fit are 4.5% N and 35.5% In for  $(\text{Ga},\text{In})(\text{N},\text{As})$  and 0.8% N for  $\text{Ga}(\text{N},\text{As})$ . The inset shows the profile over a wide angular range.

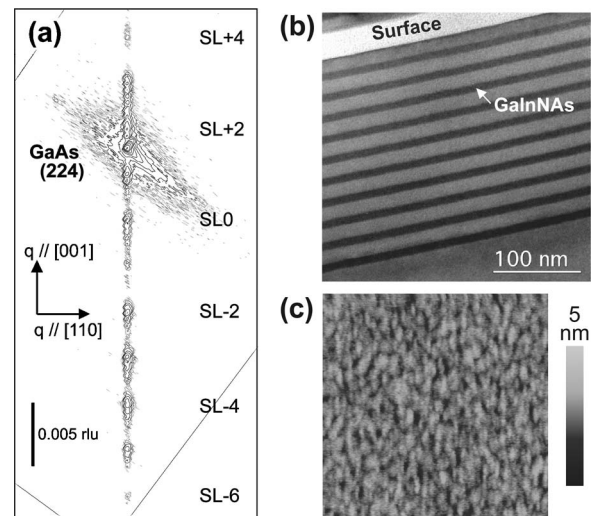


FIG. 3. Structural and morphological characteristics of the ten-period  $[(\text{Ga},\text{In})(\text{N},\text{As})$  (8 nm)/ $\text{Ga}(\text{N},\text{As})$  (14 nm)] MQW. (a) XRD reciprocal space map around the asymmetric  $\text{GaAs}(224)$  reflection, (b) cross-sectional TEM micrograph, and (c) AFM surface micrograph taken over an area of  $10 \times 10 \mu\text{m}^2$ . The root mean square roughness of this sample is 0.5 nm.

assuming a coherently strained layer structure is also shown in Fig. 2. The composition of the constituent layers is determined by taking into account the thicknesses obtained from the TEM micrograph (not shown here). As a result, we obtained 4.5% N and 35.5% In for the 3.9 nm  $(\text{Ga},\text{In})(\text{N},\text{As})$  QW and 0.8% N for the 10.8 nm  $\text{Ga}(\text{N},\text{As})$  barriers.

To obtain the desired long wavelength emission, we grew three ten-period MQWs with QW widths of 6, 7, and 8 nm, separated by 14 nm barriers. These samples were grown under identical conditions as the previous 4 nm thick MQW. XRD scans around the  $\text{GaAs}(004)$  reflection showed that these samples kept their constituents' compositions of 36% In and 4.5% N for the  $(\text{Ga},\text{In})(\text{N},\text{As})$  wells and 0.8% N for the  $\text{Ga}(\text{N},\text{As})$  barriers. The structural properties of the ten-period MQW with the 8 nm wide QWs can be deduced from the data of Fig. 3. In the XRD reciprocal space map shown in Fig. 3(a), satellite peaks with interference fringes stemming from the MQW structure can be resolved. In addition, the arrangement of those peaks along the  $[001]$  direction reveals that the constituting layers are coherently grown without strain relaxation. A cross-sectional TEM micrograph shows the regularly stacked ten QW layers which remain smooth throughout the structure. Moreover, the surface AFM micrograph taken over a  $10 \times 10 \mu\text{m}^2$  range shows a smooth surface with a root mean square roughness of 0.5 nm. These results confirm the high structural quality of this sample which is comparable to that of state-of-the-art samples grown using Sb as surfactant.<sup>3</sup>

Finally, we investigated the optical properties of the above described samples by CL at room temperature (RT). Prior to the measurements, rapid thermal annealing at 720 °C for 60 s was employed to enhance the luminescence yield. It is noteworthy that annealing up to 800 °C causes a negligible blueshift. Figure 4(a) shows RT CL spectra for the series of the ten-period MQWs with different QW widths. We observe emission in the range from 1.34 to 1.6  $\mu\text{m}$ , showing a clear redshift of the spectral peak position with increasing QW width. The larger intensities obtained for the wider (7 and 8 nm) MQWs presumably result from an enhanced electron and hole capture in the wider wells. The full

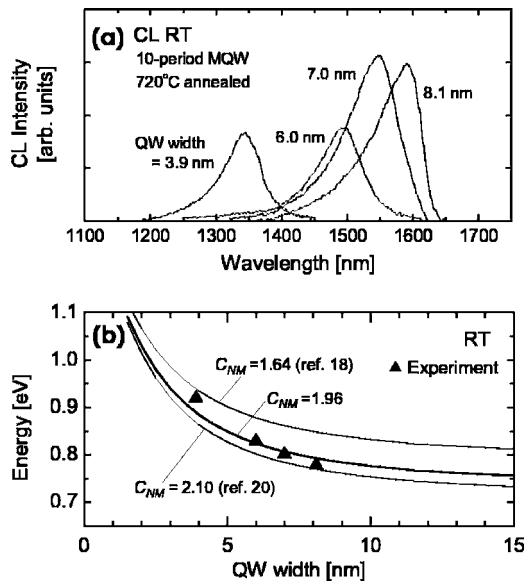


FIG. 4. (a) CL spectra for the ten-period  $\text{Ga}_{0.64}\text{In}_{0.36}\text{N}_{0.045}\text{As}_{0.955}/\text{GaN}_{0.008}\text{As}_{0.992}$  MQWs having different QW widths. The QW width obtained from the XRD fit is given for each spectrum. (b) Experimental and calculated CL peak energies vs QW width.

width at half maximums of these peaks amount to 46, 45, 48, and 42 meV for the samples with QW widths of 4, 6, 7, and 8 nm, respectively. The measured linewidth is similar to that of samples grown using Sb as surfactant.<sup>3</sup>

Next, we calculate the transition energies by solving the Schrödinger equation for finite square potential wells consisting of a (Ga,In)(N,As) well and a Ga(N,As) barrier layer.<sup>16</sup> The band gap energy and the approximated electron effective mass are calculated by using the band anticrossing (BAC) model.<sup>2</sup> According to the BAC model, the interaction between the extended host material state and the localized  $N$  state splits the conduction band into two subbands, whereby their energy for  $\text{Ga}_{1-x}\text{In}_x\text{N}_y\text{As}_{1-y}$  can be expressed by

$$E_{\pm} = \frac{1}{2}[E_M + E_N \pm \sqrt{(E_M - E_N)^2 + 4C_{NM}^2 y}]. \quad (1)$$

$E_M$  stands for the host material conduction band edge and we calculate it using the values compiled by Vurgaftman *et al.* and taking into account the strain deformation.<sup>17</sup>  $E_N$  is the energy position of localized  $N$  states, for which we use  $E_N = 1.65(1-x) + 1.44x - 0.38x(1-x)$ .<sup>18</sup>  $C_{NM}$  is the band interaction parameter depending on the In concentration, which we use as an adjustable parameter for the fit of the experimental data.<sup>16</sup> We estimate the conduction band offset  $\Delta E_C$  and the valence band offset  $\Delta E_V$  values by considering their ratios  $Q_C = \Delta E_C / (\Delta E_C + \Delta E_V)$ , which is known from the literature to be 0.9 for the GaAs/Ga(N,As) interface and 0.8 for the GaAs/(Ga,In)(N,As) interface.<sup>18,19</sup> Figure 4(b) depicts the

experimental and calculated transition energies. As a result, we obtained good agreement between experiment and calculation by using  $C_{NM} = 1.96 \pm 0.03$ , which is close to recently reported values for this material with similar In composition.<sup>16,20</sup> The observed tunability of the transition energy by varying the QW width results from the abrupt interfaces and the accurate periodicity of the samples. The calculation additionally returns  $\Delta E_C$  values of  $410 \pm 10$  meV for the (Ga,In)(N,As)/Ga(N,As) interface, which is promising for high temperature laser operation of these materials.<sup>1</sup>

In summary, we have demonstrated that a high structural and optical quality in (Ga,In)(N,As) MQWs with 36% In and 4.5% N can be obtained by MBE growth using a low As BEP and low substrate temperature. The incorporation of a high N concentration and the structural perfection of the MQWs result in RT emission ranging from 1.34 to 1.6  $\mu\text{m}$  for annealed samples by varying the quantum well width. The estimated large  $\Delta E_C$  of 410 meV is promising for high temperature operation of laser diodes.

The authors acknowledge R. Hey and L. Däweritz for their support, E. Luna and B. Satpati for TEM investigations, C. Herrman for technical assistance, and O. Brandt and Y. Horikoshi for fruitful advice.

- <sup>1</sup>M. Kondow, K. Uomi, A. Niwa, T. Kitatani, S. Watahiki, and Y. Yazawa, *Jpn. J. Appl. Phys., Part 1* **35**, 1273 (1996).
- <sup>2</sup>W. Shan, W. Walukiewicz, J. W. Ager III, E. E. Haller, J. F. Geisz, D. J. Friedman, J. M. Olson, and S. R. Kurtz, *Phys. Rev. Lett.* **82**, 1221 (1999).
- <sup>3</sup>J. S. Harris, Jr., *J. Cryst. Growth* **278**, 3 (2005).
- <sup>4</sup>J. S. Harris, Jr., *Semicond. Sci. Technol.* **17**, 1 (2002).
- <sup>5</sup>G. Jaschke, R. Averbeck, L. Geelhaar, and H. Riechert, *J. Cryst. Growth* **278**, 224 (2005).
- <sup>6</sup>G. L. Price, *Phys. Rev. Lett.* **66**, 469 (1991).
- <sup>7</sup>A. Trampert, J.-M. Chauveau, K. H. Ploog, E. Tournié, and A. Guzmán, *J. Vac. Sci. Technol. B* **22**, 2195 (2004).
- <sup>8</sup>J. Tersoff, M. D. Johnson, and B. G. Orr, *Phys. Rev. Lett.* **78**, 282 (1997).
- <sup>9</sup>J. Y. Tsao, *Materials Fundamentals of Molecular Beam Epitaxy* (Academic, San Diego, 1992), Chap. 3, p. 74.
- <sup>10</sup>K. Shiraishi, *Appl. Phys. Lett.* **60**, 1363 (1991).
- <sup>11</sup>S. Miyazawa and Y. Sekiguchi, *Jpn. J. Appl. Phys., Part 2* **30**, L921 (1991).
- <sup>12</sup>S. Zhongzhe, Y. S. Fatt, Y. K. Chuin, L. W. Khai, F. Weijun, W. Shanzhong, and N. T. Khee, *J. Appl. Phys.* **94**, 1069 (2003).
- <sup>13</sup>L. Däweritz and R. Hey, *Surf. Sci.* **236**, 15 (1990).
- <sup>14</sup>O. Brandt, P. Waltereit, and K. H. Ploog, *J. Phys. D* **35**, 577 (2002).
- <sup>15</sup>A. Krost, G. Bauer, and J. Woitok, in *Optical Characterization of Epitaxial Semiconductor Layers*, edited by G. Bauer and W. Richter (Springer, Berlin, 1995), Chap. 6, p. 287.
- <sup>16</sup>M. Galluppi, L. Geelhaar, H. Riechert, M. Hetterich, A. Grau, S. Birner, and W. Stolz, *Phys. Rev. B* **72**, 155324 (2005).
- <sup>17</sup>I. Vurgaftman, J. R. Meyer, and L. R. Ram-Mohan, *J. Appl. Phys.* **89**, 5815 (2001).
- <sup>18</sup>I. Vurgaftman and J. R. Meyer, *J. Appl. Phys.* **94**, 3675 (2003).
- <sup>19</sup>S. Tomić, E. P. O'Reilly, P. J. Klar, H. Grüning, W. Heimbrodt, W. M. Chen, and I. A. Buyanova, *Phys. Rev. B* **69**, 245305 (2004).
- <sup>20</sup>Y. N. Qiu, J. M. Rorison, H. D. Sun, S. Calvez, M. D. Dawson, and A. C. Bryce, *Appl. Phys. Lett.* **87**, 23112 (2005).